

# Dilatometric behavior and microstructure of sintered Fe–NbC and Fe–TaC composites

Antonio E. Martinelli · Domingos S. A. Paulo ·  
Rubens M. Nascimento · Michele P. Távora ·  
Uílame U. Gomes · Clodomiro Alves Jr

Received: 1 July 2004 / Accepted: 29 September 2005 / Published online: 16 December 2006  
© Springer Science+Business Media, LLC 2006

**Abstract** Fe-reinforced composites were manufactured by the addition of 10–20 wt.% NbC or TaC particles aiming at improved mechanical and wear behavior. Two varieties of Fe powders from Hoeganaes Corp. were used, Ancorsteel 1000B and 45P. Composites produced using the former variety included a small amount of Fe<sub>3</sub>P to induce liquid-phase sintering whereas 45P powder was pre-alloyed with P by the manufacturer. The hardness of the matrix was adjusted adding carbon to the composite mixture. The powders were milled for different times and annealed prior to pressing. A dilatometric study was carried out under hydrogen to establish optimum sintering profiles. Relative densities up to 97% TD were achieved. Both microstructure and density of the sintered pellets were evaluated in order to establish correlations involving composition, processing parameters and microstructure of the composite.

## Introduction

Particle reinforced metal matrix composites consist in a class of materials still under constant development. The performance of particle-dispersed composites can

be tailored to specific needs by relatively simple composition and process adjustments as compared to the development of particle-precipitated composites and new steels. In particular, the dispersion of hard ceramic particles into steel matrixes potentially increases specific resistance at room and high temperatures in addition to improve wear resistance and dimensional stability. The coefficient of thermal expansion of composites can also be adjusted to reduce misfits when joining to other metals or ceramics is required [1]. Mainly as a result of such intrinsic properties, composite materials have been increasingly used in the production of high-performance mechanical components at competitive prices [2]. In particular, reinforced steels have been used in the automotive and textile industry, as well as in the fabrication of high-speed cutting tools and grinding media [3].

The properties of sintered composites are determined not only by the nature and quality of the raw materials employed but also by the microstructure and porosity resulting from the processing techniques and thermal sintering profile. Therefore, understanding the dilatometric behavior and sintering mechanism consist in necessary steps towards the development of particle-dispersed composites from any combination of matrix and reinforcement materials [4]. The role of important processing stages including milling and sintering as well as material selection have been extensively studied since they determine the final microstructure responsible for the adequacy or not of a particular composite material for an intended application [5–7]. The selection of improved metallic powders, presently available, can also be used as tools to tailor the properties of reinforced steels. Pre-alloyed steels with controlled particle morphology and size distribution can be useful

---

A. E. Martinelli (✉) · D. S. A. Paulo ·  
R. M. Nascimento · M. P. Távora · U. U. Gomes ·  
C. Alves Jr  
Departamento de Química, Laboratório de Cimentos,  
Universidade Federal do Rio Grande do Norte, Av.  
Senador Salgado Filho, S/N, Lagoa Nova, CEP 59.072-970  
Natal, RN, Brasil  
e-mail: aemart@uol.com.br

in assisting composite homogenization and densification [8]. Powdered metallic composite materials have been manufactured to emulate or exceed the properties depicted by conventional metal alloys manufactured by rolling, forging or drawing [9, 10]. Different combinations of Fe-based matrixes and hard ceramic powders have been studied aiming at composite materials with properties similar to those of conventional tool steels [11, 12]. Carbides such as NbC, TaC, VC and TiC have been combined to Fe or steel powders in the manufacture of sintered composites [13]. Niobium carbide and tantalum carbide are hard ceramic powders that can be produced from minerals commonly encountered in Northeastern Brazil. They can be used for structural ends either in the production of refractory bulk components or as reinforcement in particle-dispersed steels [14].

The main goal of the study reported herein was to access the potential of such hard ceramics to reinforce steels by establishing the milling and sintering parameters necessary to obtain dense composites. The dilatometric behavior and final microstructure of the sintered materials are particularly emphasized in the discussion.

## Experimental procedure

The raw materials used in the composite production consisted in Ancorsteel 1000B (D50 = 92  $\mu\text{m}$ , wt.% P = 0.005%) and 45P (D50 = 40  $\mu\text{m}$ , wt.% P = 0.45%) Fe powders supplied by Hoeganaes Corporation. NbC (D50 = 2  $\mu\text{m}$ ) and TaC (D50 = 9  $\mu\text{m}$ ) powders from H.C. Starck, Germany, were added as reinforcement. The morphology of the starting ceramic powders was observed by scanning electron microscopy (SEM). Graphite was used to adjust the hardness of the matrix and Fe<sub>3</sub>P as liquid phase additive in composites produced using Ancorsteel 1000B. A summary of the composite compositions produced in the scope of the present study is shown in Table 1. The composite powders were wet-milled in a planetary mill at 300 rpm during 10 h (composites labeled A) or 20 h (composites labeled B). After milling, the powder mixtures were annealed at 800 °C for 1 h under flowing hydrogen and pressed into cylindrical pellets under 600 MPa.

A dilatometric study was then carried out under hydrogen. The heating rate was set to 10 °C/min and the soaking time at the sintering temperatures listed in Table 2 was either 30 or 60 min. Both apparent green and sintered densities were evaluated. The relative density of the composites was estimated using the calculated theoretical densities of Fe–10%NbC

**Table 1** Composition of the composites (wt.%)

| Composition | (%) NbC | (%) TaC | (%) C | (%) Fe <sub>3</sub> P | (%) Fe 1000B | (%) Fe 45P |
|-------------|---------|---------|-------|-----------------------|--------------|------------|
| 1           | 10.0    | –       | 1.0   | 1.5                   | 87.5         | –          |
| 2           | 20.0    | –       | 1.0   | 1.5                   | 77.5         | –          |
| 3           | –       | 10      | 1.0   | 1.5                   | 87.5         | –          |
| 4           | 10.0    | –       | 1.0   | –                     | –            | 89.0       |
| 5           | –       | 10.0    | 1.0   | –                     | –            | 89.0       |

**Table 2** Thermal profile parameters

| Composite label | Upper temperature (°C) | Soaking time (min) |
|-----------------|------------------------|--------------------|
| 1A              | 1,240                  | 60                 |
| 1B              | 1,250                  | 60                 |
| 2A              | 1,180                  | 30                 |
| 2B              | 1,180                  | 30                 |
| 3A              | 1,180                  | 30                 |
| 3B              | 1,180                  | 30                 |
| 4A              | 1,180                  | 30                 |
| 4B              | 1,180                  | 30                 |
| 5A              | 1,180                  | 30                 |

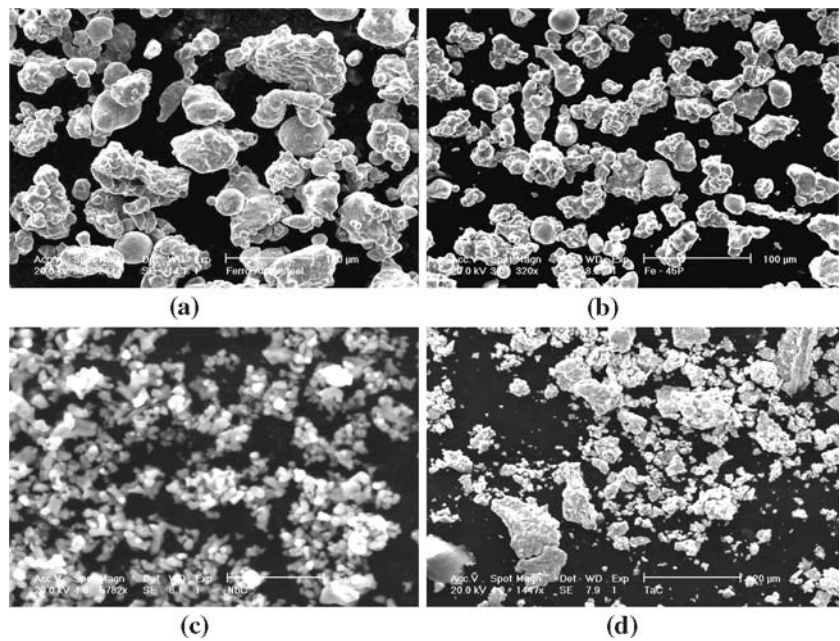
(7.879 g/cm<sup>3</sup>), Fe–20%NbC (8.104 g/cm<sup>3</sup>) and Fe–10% TaC (8.528 g/cm<sup>3</sup>). Microstructural analyses were carried out using a Olympus optical microscope and a Philips XL30 ESEM system equipped with a secondary electron detector, a back-scattered electron detector and a EDS detection and analysis system.

## Results and discussion

The morphology of the powders used in composite manufacture is shown in Fig. 1. Fe1000B consisted of irregularly shaped agglomerates of average diameter ~100  $\mu\text{m}$ . Fe45P depicted similar morphology, although the size of the agglomerates was roughly half of that observed for Fe1000B. NbC and TaC consisted of slightly rounded and angular particles, respectively. Milling at 300 rpm during 20 h resulted in adequate homogenization of the composite powder mixture since a substantial fraction of hard ceramic particles was mechanically interlocked with the relatively larger Fe particles.

The SEM image shown in Fig. 2 depicts composite particles produced by milling. They consist of hard NbC particles adhered to the surface of larger Fe particles. The relatively high milling energy obtained in the planetary mill assisted in the formation of composite particles, whose number increased by increasing the angular speed of the mill from 300 to 600 rpm. Nevertheless, significant concentrations of carbide particles were still observed at the grain boundaries of sintered pellets. Concerning the sintering behavior,

**Fig. 1** Morphology of (a) Fe1000B; (b) Fe45P; (c) NbC and (d) TaC powders



no significant changes were observed in the dilatometric behavior of the composites as a function of the milling time, probably because the milled powders were annealed prior to compaction. A representative dilatometric plot of a composite milled for 20 h (composite 2B) is shown in Fig. 3.

Upon heating,  $DI/I_0$  was the net result of two opposing mechanisms, i.e., linear thermal expansion and pore closing. Up to  $\sim 600^\circ\text{C}$  (region I), the composite expanded due to limited retraction rates characteristic to surface diffusion. The first necks could be observed. As the temperature increased, grain boundary and volumetric diffusion became the dominant mechanisms, as suggested by a slight change in the slope of the plot from region I to region II. The thermal expansion was roughly counterbalanced by the retraction rate. Within the temperature range that limited regions I and II, the matrix of the composite depicted the BCC crystal structure. Further heating to around  $900^\circ\text{C}$  was characterized not only by sintering but also homogenization with mutual diffusion of P

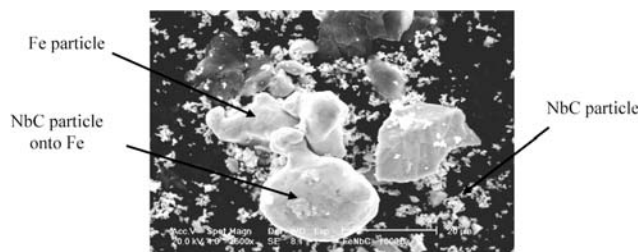


**Fig. 2** SEM image of Fe-10%NbC powder after milling for 10 h

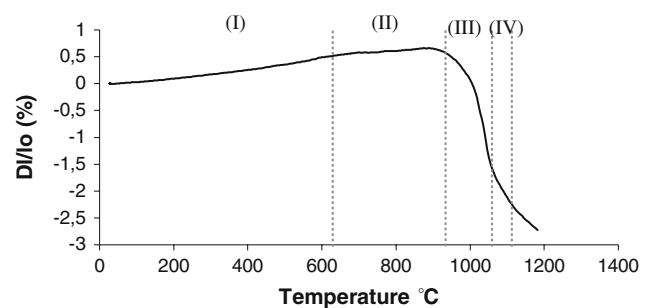


**Fig. 3** Dilatometric plot of composite 2B

from  $\text{Fe}_3\text{P}$  into Fe particles and Fe atoms into  $\text{Fe}_3\text{P}$ . Carbon is also expected to diffuse into the Fe matrix. From  $900^\circ\text{C}$  to  $1,000^\circ\text{C}$ , the retraction rate increased due to the  $\alpha \rightarrow \gamma$  transformation of the Fe matrix (region III). Subsequently, the onset of liquid phase sintering can be noticed around  $1,150^\circ\text{C}$  and was responsible for the final densification of the composite (region IV). No significant changes were observed in the dilatometric behavior of Fe–NbC composites as a function of NbC contents. On the other hand, the concentration of  $\text{Fe}_3\text{P}$  (liquid phase additive) determined the amount of liquid formed and, consequently, the sintering rate, final microstructure and properties of the sintered pellets.

In the formulation of composites 3A and 3B, NbC was replaced by TaC. Not only the average particle size of TaC ( $9\ \mu\text{m}$ ) was larger than that of NbC ( $2\ \mu\text{m}$ ), but also the distribution itself was wider than that of NbC.  $D_{90}/D_{50}$  was equal to 2.5 for NbC and 5.6 for TaC. As a result, limited homogenization of TaC particles in the

iron matrix could be expected upon milling, which could affect the sintering kinetics and final microstructure of the composite. The dilatometric behavior of composite 3B (Fe-10%TaC milled for 20 h) is shown in Fig. 4. From ambient to approximately 650 °C, a slight expansion was noticed and ruled by a mechanism similar to that discussed for composite 2. The slope of the dilatometric plot changed in the range of 650–800 °C, corresponding to the onset of the contraction process. The slope in region (II) of the plot may have been determined by the rupture of the surface oxide layer of the particles in addition to gradual development of the  $\gamma$ -phase typical of the hypereutectoid steel. Region (III), between 800 °C and 900 °C, was characterized by volumetric diffusion and  $\alpha \rightarrow \gamma$  transformation. Liquid phase was formed around 1,000 °C, resulting in rapid contraction. The differences encountered in the dilatometric characteristics of composites containing TaC with respect to those containing NbC may be related to the particle size distribution resulting from milling. In addition, the density of TaC (14.5 g/cm<sup>3</sup>) is roughly double that of Fe or NbC (~7.5 g/cm<sup>3</sup>), which may have considerably impaired the homogeneity of the mixture upon milling.

The dilatometric plot corresponding to composite 4A (Fe45P-10%NbC) is illustrated in Fig. 5. The shape of the curve did not indicate the occurrence of liquid phase sintering, which is consistent with the use of 45P Fe powder and no liquid phase additive. The composite slightly expanded up to 550 °C, at which point the slope of the curve changed, characterizing an increase in the sintering rate. Around 1,000 °C, the retraction rate further increased, probably due to extended volumetric diffusion. An overview of the density values obtained by sintering different composites is shown in Table 3. Densification values ranging from 92% to 97% TD were achieved and reveal the possibility of obtaining sintered NbC- and TaC-reinforced steels for practical applications.

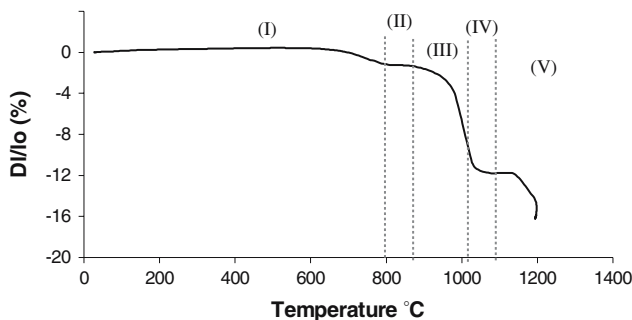


Fig. 4 Dilatometric plot of composite 3B

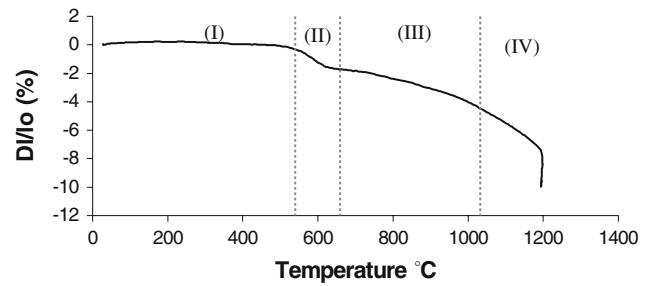


Fig. 5 Dilatometric plot of composite 4A

Table 3 Relative density of sintered composite pellets

| Composite label | Sintering temperature (°C) | Relative density (% TD) |
|-----------------|----------------------------|-------------------------|
| 1A              | 1,240                      | 94                      |
| 1B              | 1,250                      | 97                      |
| 2A              | 1,180                      | 94                      |
| 2B              | 1,180                      | 95                      |
| 3A              | 1,180                      | 92                      |
| 3B              | 1,180                      | 96                      |
| 4A              | 1,180                      | 93                      |
| 4B              | 1,180                      | 95                      |
| 5A              | 1,180                      | 92                      |

The final microstructure of composite 1B (Fe-10%NbC milled for 20 h), and sintered at 1,260 °C for 60 min is shown in Fig. 6. Virtually no porosity could be observed (relative density 97% TD). Carbide particles were uniformly distributed throughout the matrix, although agglomerates could be observed at grain boundaries. Areas characterized by the former presence of extensive liquid phase could also be observed, thus confirming the results obtained from the dilatometric study. Due to the relatively high sintering temperature used, excessive contents of liquid phase affected the dimensional stability of the pellets.

Micrographs corresponding to composites 2 (Fe 1000B-20%NbC) milled for different times are shown in Fig. 7. The microstructure of composite 2B, milled for 20 h, revealed better homogenization in the distribution of NbC particles comparing to composite 2A, milled for 10 h. In this case, the carbide particles were

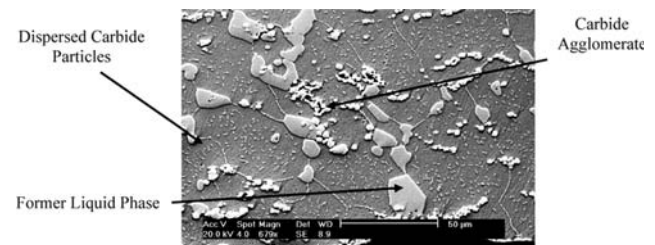
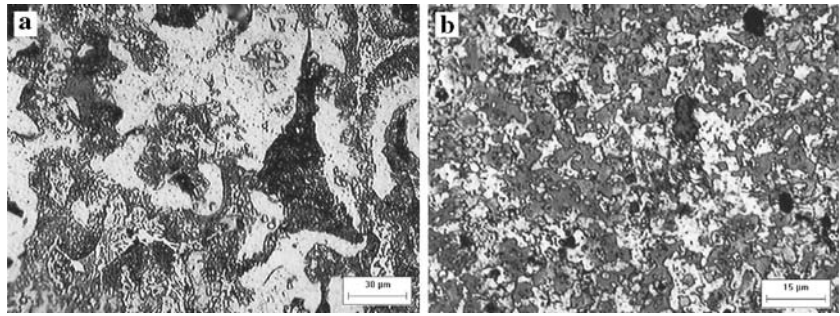


Fig. 6 SEM image of composite 1B



**Fig. 7** Optical micrograph of composite (a) 2A and (b) 2B. Detail on the refined grain structure and homogeneous distribution of carbide particles



preferentially located in specific areas of the microstructure, especially grain boundaries. The concentration of reinforcing particles at grain boundaries is deleterious to the performance of the composite as differences especially in hardness are observed along the microstructure of a composite component. The microstructure of composite 3B (10% TaC—milled at 300 rpm/20 h) is shown in Fig. 8. The carbide particles were homogeneously distributed with little agglomeration at grain boundaries. In addition, using the parameters obtained from the dilatometric experiments, densification up to 96% TD with no effect on the dimensional stability of the pellets was achieved.

Composites produced using 45P Fe powder (pre-alloyed with P) did not reveal any signs of liquid phase formation. Solid state sintering was the dominant densification mechanism, as clearly suggested by the dilatometric study. A typical microstructure of this kind of material is shown in Fig. 9. The carbide particles were also homogeneously distributed along the matrix with little agglomeration at grain boundaries. Moreover, little porosity can be observed, since the relative density of this material was ~ 97% TD.

## Conclusions

(1) Composites produced using Fe1000B and milled for 20 h could be substantially densified to close porosity and depicted homogeneous distribution of carbide particles along the matrix.

**Fig. 8** SEM images of composite 3B. (a) Back-scattered electron image detailing uniform distribution of TaC particles; (b) secondary electron image showing perlite grain, carbide particles precipitated in grain boundary, solidified liquid phase and residual porosity

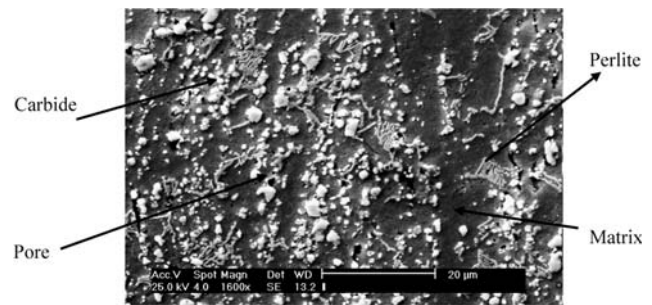
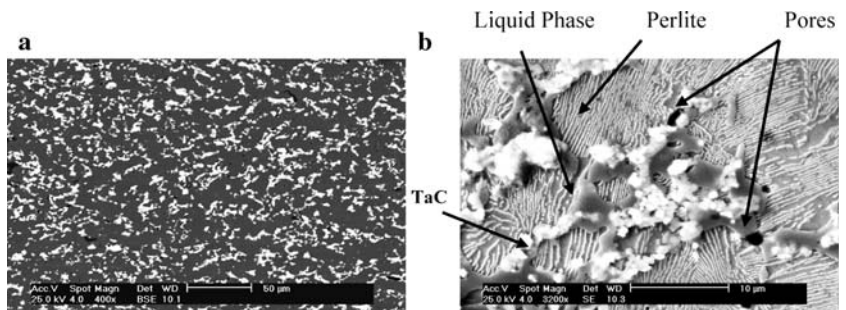


**Fig. 9** SEM image of microstructure of composite 4A

- (2) The number of carbide particles mechanically interlocked with Fe 1000B particles was greater than with Fe 45P. This was probably because Fe 45P particles were smaller and harder than the Fe 1000B ones.
- (3) The dilatometric behavior of Fe–NbC composites was not qualitatively or quantitatively affected by the contents of NbC particles added as reinforcement.
- (4) Composites produced using Fe 1000B and Fe<sub>3</sub>P sintered assisted by liquid phase whereas solid state sintering was the mechanism responsible for sintering Fe 45P based composite compositions.
- (5) Relative density values ranging from 92% to 97% DT were obtained and corresponded to Fe–NbC and Fe–TaC composites sintered to close porosity.

**Acknowledgements** The authors express their gratitude to Prof. Alosio Nelmo Klein of the Universidade Federal de Santa Catarina, Brazil, for the use of the Materials Laboratory (LABMAT) facilities.

## References

1. Cizeron G (1994) *Rev de Metall* 91(5):683
2. Mitkov M (1994) *Sci Sinter* 26(2):173
3. Eckert J (1994) *Int J Refract Met Hard Mater* 12(6):335
4. Cho WS, Hayashi K (1994) *J Jpn Soc Heat Treat* 34(4):184
5. Imiduk DMD (1996) *J Metals* 48(1):33
6. Takata J, Kawai N (1995) *Powder Metall* 38(3):209
7. Mizuno Y (1995) *Powder Metall* 37(3):191
8. Lei Z (1995) *PM Technol* 13(1):26
9. Gaebel R (1996) *Acta Mater* 44(8):3215
10. Rutz HG, Hanejko FG (1995) *Int J Powder Metall* 31(1):9
11. Sridharan K, Perepezko JH (1994) *Int J Powder Metall* 30(3):301
12. Engstrom U (1996) *Powder Metall* 39(1):37
13. Torralba JM (1995) *Rev de Metall* 3(1):14
14. Ristic MM (1994) *Sci Sinter* 26(2):89